Glutamate cycle changes in the putamen of patients with de novo Parkinson's disease using 1H MRS

Carine Chassain, Aurélie Cladiere, Camille Tsoutsos, Bruno Pereira, Fawzi Boumezbeur, Bérangère Debilly, Ana-Raquel Marques, Stéphane Thobois, Franck Durif

Version of Record: https://www.sciencedirect.com/science/article/pii/S1353802022001341
Manuscript_49452e18318f4fc188c74912483c694b

Glutamate cycle changes in the putamen of patients with *de novo* Parkinson's disease using ^{1}H MRS

Authors: Carine CHASSAIN[1], Aurélie CLADIERE[1], Camille TSOUTSOS[1], Bruno PEREIRA[2], Fawzi BOUMEZBEUR[3], Bérangère DEBILLY[1], Ana-Raquel MARQUES[1], Stéphane THOBOIS[4], Franck DURIF[1]

[1] *University of Clermont Auvergne, CHU, CNRS, Clermont Auvergne INP, Institut Pascal, F-63000 Clermont-Ferrand*
[2] *CHU Gabriel Montpied, Clinical Research Department, Biostatistics Unit, 63000 Clermont-Ferrand*
[3] *NeuroSpin, Frederic Joliot Institute, CEA, Université Paris-Saclay, CNRS, UMR BAOBAB, 91191 Gif-sur-Yvette, France*
[4] *Université de Lyon, université Claude-Bernard Lyon I, faculté de médecine Lyon Sud Charles-Mérieux, Lyon, France; Hospices civils de Lyon, hôpital neurologique Pierre-Wertheimer, service de neurologie C, centre expert parkinson, Lyon, France; CNRS, Institut des sciences cognitives Marc Jeannerod, UMR 5229, 69675 Bron*

Corresponding author: Dr Carine Chassain, CHU Gabriel Montpied, MRI department, 63000 Clermont-Ferrand, France

Email : carine.chassain@inrae.fr; phone : +33473178455

Running title: ^{1}H MRS to follow Parkinson's disease

Word count: Abstract: 242 words; Manuscript body (including of introduction, methods, results and discussion): 4,065 words.

Abbreviations used: CSD, chemical shift displacement; Cho, choline; Cr, creatine; CRLB, Cramér-Rao lower bounds; FOV, field of view; GABA, γ-aminobutyric acid; Glc, glucose; Gln, glutamine; Glu, glutamate; Glx, pool glutamate + glutamine; GPC: glycerophosphocholine; Ins, inositol; MRI, magnetic resonance imaging; ^{1}H-MRS, proton magnetic resonance spectroscopy; tNAA, N-acetyl-aspartate + N-acetyl-aspartyl-glutamate; PCr, phosphocreatine; PD, Parkinson's disease; SEM, standard error of the mean; SD, standard deviation; SNpc, substantia nigra pars compacta; SNR, signal to noise ratio; STN, subthalamic nucleus; Tau, taurine; TE, echo-time; TI, inversion time; TR, repetition time; VOI, volume of interest.

Manuscript type:

Full length article

Relevant conflicts of interest/financial disclosures:

The authors have no conflict of interest to report

Funding sources:

Internal grant of the University Hospital of Clermont-Ferrand.

HIGHLIGHTS

- MRS assesses glutamate, glutamine levels from the putamen of *de novo* parkinsonian patients
- Glutamate, glutamine levels are higher in the putamen ipsilateral to clinical signs
- Abnormalities in Glutamate metabolism therefore occur early in Parkinson Disease
- However, changes occur unexpectedly in the putamen of the less damaged hemisphere
- Metabolic changes are not dependent solely on dopamine loss

ABSTRACT

Introduction: To investigate glutamatergic metabolism changes in the putamen of patients with *de novo* Parkinson's Disease (PD) and test the hypothesis that glutamate (Glu) levels are abnormally elevated in the putamen contralateral to where the motor clinical signs predominate as expected from observations in animal models**.**

Methods: ^{1}H NMR spectra from 17 healthy control volunteers were compared with spectra from 17 *de novo* PD patients of who 14 were evaluated again after 2-3 years of disease progression. Statistical analysis used random-effects models.

Results: The only significant difference between PD patients and controls was a higher glutamine (Gln) concentration in the putamen ipsilateral to the hemibody with predominant motor signs (Visit 1: 6.0±0.4mM vs. 5.2±0.2mM, $p<0.05$; Visit 2: 6.2±0.3mM vs. 5.2±0.2mM, $p<0.05$). At Visit 1, PD patients had higher Glu and Gln levels in the putamen ipsilateral versus contralateral to dominant clinical signs (Glu: 12.2±0.6mM vs. 10.4±0.6mM, $p<0.05$; Gln: 6.0±0.4mM vs. 4.8±0.4mM, $p<0.05$; Glu and Gln pool (Glx): 17.9±0.8mM vs. 14.7±1.1mM, $p<0.05$). At Visit 2, the sum of the two metabolites remained significantly higher in the ipsilateral versus contralateral putamen (Glx: 18.3±0.6mM vs. 16.1±0.9mM, $p<0.05$).

Conclusion: In *de novo* PD patients, the putamen ipsilateral to the more affected hemibody showed elevated Gln versus controls and elevated Glu and Gln concentrations versus the contralateral side. Abnormalities in Glu metabolism therefore occur early in PD but unexpectedly in the putamen contralateral to the more damaged hemisphere, suggesting they are not dependent solely on dopamine loss.

Keywords: Parkinson's disease, ^{1}H magnetic resonance spectroscopy, putamen, glutamate, glutamine

INTRODUCTION

Parkinson's disease (PD) is a common neurodegenerative disorder characterised mostly by the degeneration of dopaminergic neurons in the substantia nigra, leading to the classical bradykinesia-rigidity-tremor triad [1]. The degeneration of the nigrostriatal dopaminergic neurons causes dysfunction of the cortico-basal ganglia-cortical loops and reactive changes in striatal neurotransmission. In particular complex remodelling occurs at the synapses formed by the cortical afferents onto the striatal projection neurons, also called medium-sized spiny neurons, suggesting altered glutamatergic transmission. Data from studies in animal models consistently show a decrease in the spine density of striatal projection neurons, but there is no consensus on the changes in the number of glutamatergic terminals [2]. However, data argue for increased transmission at the remaining glutamatergic synapses. Analysis of the morphological characteristics of the asymmetrical synapses formed by putative corticostriatal glutamatergic afferents onto dendritic spines of neurons revealed an increase in the diameter of the post-synaptic area and the number of perforated synapses in the caudate nucleus of PD patients [3] as well as in the non-human primate MPTP PD model [4]. Slice electrophysiological studies have found evidence for increased corticostriatal transmission and loss of form of plasticity, long-term potentiation (LTP) and long-term depression (LTD), or of LTD depending on the extent of striatal dopamine denervation in 6-hydroxydopamine (6-OHDA)-induced rodent models of PD [5,6]. Finally, other works has reported increased or unchanged extracellular levels of glutamate (Glu) as determined by *in vivo* microdialysis in rat PD models [7].

In vivo proton (^{1}H) magnetic resonance spectroscopy (MRS) could offer a useful tool to validate the hypothesis of reactive changes in striatal glutamatergic transmission in response to dopaminergic denervation. MRS can be used to detect and quantify several brain metabolites, among which intracellular + extracellular pools of neurotransmission-related metabolites, GABA (γ-aminobutyric acid), Glu and glutamine (Gln). MRS also provides information about neuronal integrity (N-acetyl-aspartate + N-acetyl-aspartyl-glutamate, tNAA), membrane turnover (glycerophosphocholine +

phosphocholine, tCho), gliosis (myo-inositol, Ins) and energy metabolism (creatine + phosphocreatine, tCr). Previously, we conducted ^{1}H MRS studies on toxin-induced PD models in mice and rats and reported changes in several metabolites in the striatum and the substantia nigra, which are respectively main input and output structures of the basal ganglia network, among which increased striatal levels of GABA, Glu and Gln [8,9,10]. Interestingly, the dopamine lesion-induced neurochemical profiles were normalised by the acute administration of L-dopa [8] while showing complex evolution under acute, subchronic (7 days) or chronic (5 weeks) deep brain stimulation of the subthalamic nucleus (NST) [9,10].

Numerous ^{1}H MRS studies have investigated local metabolic changes in patients suffering from PD [11-13]. Different brain structures of interest have been explored, such as the motor cortex [12], the posterior cingulate gyrus [12], the temporo-parietal cortex [13], the occipital lobe [13], and the substantia nigra [11]. In cortical structures, these studies reported lower tNAA/tCr ratio in PD patients than in age-matched controls from early disease stages [12,13]. Regarding the putamen, we previously observed that patients with moderate PD in drug-off condition had lower levels of m-Ins and of tNAA versus control subjects, which could reflect early osmotic changes in astrocytes and impaired mitochondrial energy metabolism, respectively [14]. The dopaminergic treatment normalized m-Ins and tNAA levels. Data concerning Glu and Gln concentrations are conflicting, showing either no change [14,15] or increases [16] in the putamen of advanced stage PD patients. Such discrepancies could be due to differences in patients' clinical profiles, such as disease duration and treatments received. On the other hand, most of our knowledge from experimental animals comes from late disease stage models, based on extensive dopamine lesions, which do not recapitulate the complex progressive neurodegenerative process that affects multiple neuronal systems besides the nigrostriatal pathway in PD.

Here, we used MRS to obtain an overview on glutamate metabolism abnormalities in the putamen ipsi and contralateral to the more affected hemibody in *de novo* drug-naïve PD patients and to follow their evolution after two to three years of disease progression. This would tell us determining

whether these metabolite levels were correlated to clinical signs and so could be considered as biomarkers reflecting disease progression.

METHODS

Subjects. This prospective imaging study included 20 treatment-naïve *de novo* PD patients and 20 healthy age and sex-matched subjects with no history of neurological disorders. PD patients were recruited at two sites (Movement Disorders Departments of the University Hospitals of Clermont-Ferrand and Lyon), by movement disorder specialists (FD, ST). Inclusion criteria were: idiopathic PD according to the UK PD Brain Bank criteria for idiopathic PD [17] and less than 5-year disease duration, Hoehn and Yahr stage =1-2, no dopaminergic treatment. PD patients with severe rest tremor (>3 on one sub-item of UPDRS) and dementia (as assessed by DSM-IV criteria) were not recruited. Healthy volunteers were recruited from a healthy volunteers' list of the Clinical Investigation Centre of Clermont-Ferrand University Hospital. For both groups, MRI contraindications and any medication that could interact with brain neurotransmitters (antidepressant, neuroleptics) were criteria for exclusion.

The protocol was approved by the Regional Medical School Ethics Committee and registered under number 2010-021202-38. All healthy volunteers and PD patients gave their informed consent in compliance with the French national health regulations and the Declaration of Helsinki guidelines.

PD patients were screened during an outpatient visit in each Neurological Department (FD, Clermont-Ferrand; ST, Lyon). They were qualified at the Radiology Department of the University Hospital in Clermont-Ferrand for their MRI in the morning (8 a.m.). The total Unified Parkinson's Disease Rating Scale (UPDRS) was then applied by a neurologist specialised in movement disorders (FD) to evaluate the severity of the disease. The following items of the UPDRS part III motor section were scored for left and right side: rigidity, bradykinesia, and rest and postural tremor. The body side with the higher scores for these items was the more affected hemibody.

Among the 20 *de novo* PD patients, three were excluded of the study. One patient was reclassified as possible multiple system atrophy (MSA) and two patients developed cognitive disorders

compatible with possible Lewy body disease. Seventeen patients and the seventeen age and sex-matched control subjects were finally includes at baseline. The same protocol was applied after 2-4 years evolution in 14/17 patients (Table 1, delay between visit 1 and visit 2 was 36.9±7.7 months and values were ranged between 27 and 48 months). Among the three patients who did not continue the protocol, one subject did not wish to continue the study, and two others were lost to follow-up. During the follow-up, the 14 patients received dopamine agonists and three out of these 14 patients also started levodopa. L-Dopa equivalent daily dose (LEDD) was calculated according to previous literature and was equal to 444±52 mg/day [18]. The MRI exam and clinical evaluation were done under chronic treatment between 1h and 2 h after taking the first dose of the medication. Healthy volunteers were examined only once.

MRI and MRS acquisition.

MRI and ^{1}H MRS examinations were performed on a GE 3T MR750 scanner (GE Medical Systems, Milwaukee, WI) using a 32-channel head coil. Foam padding and paper tape was used to restrict motion within the scanner. To position the voxels, conventional anatomical images were acquired using a 3D T_1 Inversion Recovery sequence [TR (repetition time) =8.8s, TE (echo time) =3.5ms, TI (inversion time) =400ms, slice thickness =1.2 mm, FOV (field of view) =24 cm, flip angle= 12°, NEX (number of excitations) =1, resolution =288×288]. Slices were aligned along the anterior commissure-posterior commissure (ACPC) line.

Two 4.5mL spectroscopic voxels (dimensions = 10mm×30mm×15mm) were positioned over the left and right putamen respectively as shown in Fig. 1. A point-resolved spectroscopy sequence was used for localisation (PRESS: TR =1.5 s, TE =29 ms, 512 scans, spectral bandwidth =5000 Hz, 4096 complex data points), combined with a CHESS water suppression scheme. Radio frequency (RF) pulses/gradient slice selection such as PRESS exhibit a localization inaccuracy as chemical shift displacement (CSD) [19]. The effective bandwidth of the RF pulses used here was 2367 Hz and the CSD for the volume of interest (VOI) was around 19% in all plans. To achieve the most accurate localization and to reduce the CSD, the OVERPRESS method was used [19]. The excited

volume was deliberately chosen to be in the order of 20% larger than the VOI and selective suppression pulses (outer-volume suppression bands) were used to redefine the desired smaller region minimal CSD. Following automatic shimming, an unsuppressed water spectrum was acquired as an internal reference of concentration before the neurometabolic profiles were acquired. A water suppression efficiency of 95% and a spectral line width below 13 Hz for the unsuppressed water signal were considered acceptable. To check that the boundaries of the right and left putamen voxels encompassed the desired region, a quality control was performed using Statistical Parametric Mapping software (SPM12, Welcome Trust Centre for neuroimaging, London, UK, http://www.fil.ion.ucl.ac.uk/spm/) implemented in Matlab 2018a. Briefly, 3D T1-weighted anatomical images was segmented and normalized to the MNI152 space with the DARTEL algorithm. We visualized that the boundaries of the voxels encompassed the putamen using xjview toolbox and Talairach Daemon Labels. Then, to evaluate the reproducibility of the voxel positioning between the two MRS sessions for each PD patient, percentage voxel overlap was estimated using Gimp2.6.11. Briefly, for the three acquisition planes, one image acquired during the first MRI was opened and the image acquired during the second exam was opened as a layer. The two images were normalised according to grey levels using the Gimp image registration toolbox (transformation model, shift and rotate). By transparency, the two-voxels overlay were then used to estimate percentage of voxel coverage.

MRS analysis. All spectra were processed using LCModel software version 6.3 (Provencher, Oakville, Ontario, Canada) [20] which uses Bayesian analysis starting with a simulated basis set of metabolites and macromolecules to provide estimates of metabolite and macromolecule concentrations without operator bias. The following metabolites were included in the basis set: alanine (Ala), aspartate (Asp), phospho- choline (PCh), creatine (Cr), phosphocreatine (PCr), γ-Aminobutyric acid (GABA), Glu, glutamine (Gln), glutathione (GSH), myo-inositiol (Ins), Lac, NAA, N-acetyl-aspartateglutamate (NAAG), glycerophospho- choline (GPC), glucose (Glc), scyllo-inositol (Scyllo) and taurine (Tau). Both Glu, Gln and Glx (pool glutamate + glutamine) were

reported throughout, since Glx remains a more robust metric than Glu at 3T. Analyses were performed blindly by CC. Analysis was carried out for each set of spectra from the right and left putamen for each patient. Spectra were considered in the final analysis based on quality criteria defined by objective output parameters from the LCModel analysis, i.e. sufficient spectral resolution (line width < 0.10 ppm, thus < 12.77 Hz), and residuals that were randomly scattered about zero to indicate a reasonable fit. The signal-to-noise ratio (SNR) was evaluated as the intensity of the N- acetyl-aspartate (NAA) singlet resonance at 2.01 ppm divided by the standard deviation (SD) of the noise between 9.5 and 10 ppm. Metabolites which were quantified with a relative Cramer Rao Lower Bound (CRLB) above 20% were excluded from further statistical analyses. For metabolite quantification, the unsuppressed water signal was used as an internal reference of concentration, assuming a typical water concentration of 43.3 M in grey matter and a 100% visibility of the water signal. The neurochemical concentrations were not corrected for the negligible volume fraction of cerebrospinal fluid nor for the moderate differential T_1 and T_2 weightings between metabolites and water. Values are expressed as mean ± standard error of the mean (SEM) in mM.

Statistical analysis.

Continuous data are presented as means and standard error of the mean (SEM). The assumption of normality was assessed using the Shapiro-Wilk and Agostino tests. The comparisons of clinical data (i.e. between visit 1 an visit 2 for PD) were performed using a paired Student's t-test. Results were expressed using mean ± SEM and t-values from statistical test. The comparisons of absolute concentrations of metabolites between healthy subjects and PD were conducted using random-effects models in order to take into account matching (pair as random-effect). Age and gender were considered as adjustment covariates. Random-effects models were also used to compare absolute concentrations of metabolites early and after 2-3 years of disease progression, only for PD patients, in order to take into account between and within patient variability and between and within side effect (patient and side as random-effects). Time, side and time x side interaction were assessed.

Results were expressed using mean ± SEM and z-values from random-effect models. Duration of disease and UPDRS III were considered as adjustment covariates. The relationships between continuous data were studied by computing correlation coefficients, Pearson or Spearman according to statistical distribution. Šidák type-I error correction was applied for multiple comparisons. Statistical analysis was performed using Stata 15 software (StataCorp LP, College Station, TX). $P < 0.05$ indicates a statistically significant difference

RESULTS

Participants.

The Hoehn and Yahr stage of PD subjects was lower than 2 with a mean disease duration of 18 months at the inclusion visit. Motor signs predominated on the right -side in thirteen patients (76%), and on the left side in three patients (18%) and were symmetrical for one patient. For the PD patient with no dominantly affected body side, the right UPDRS-III motor sub-score was 8 and the left was 7. Then we decided to pool this patient with others with right side of PD onset. At baseline, patients displayed a mean UPDRS part III score of 14.8 points (SEM 2.1, min 5, max 28). There was no significant difference in motor severity between the two visits. Motor signs predominated on the same side at baseline and visit 2. The detailed characteristics of the patients are summarized in Table 1.

Spectral quality.

A typical neurometabolic profile of the putamen and its spectral decomposition using LCModel is shown in Fig. 2. The figure shows a spectrum from a control subject and the corresponding LCModel spectral fit. Fit residual, some individual metabolites and macromolecules fits and baseline are presented. For all groups, the fit successfully quantifies the following metabolites with CRLB < 5%: Glu, tNAA (sum of NAA and NAAG), tCho (sum of GPC and PCh), tCr (sum of Cr and PCr), and Glx and with CRLB < 20%: GABA, Gln, Tau, Ins. The average SNR was 19 ± 4 for the control group, 18.9±4.2 for PD patients at visit 1 and 19.3±4.5 at visit 2. The linewidth (FWHM) was also stable between groups, it was 0.107±0.002 ppm for the control group,

0.102±0.001 ppm for PD patients at visit 1 and 0.105±0.002 ppm at visit 2 (corresponding to approximately 13 Hz).

Neurochemical profiles.

The reproducibility of the voxel positioning between the two MRS sessions for each PD patient, assessed by the percentage voxel coverage, was considered correct. On average across the cohort of PD patients, the voxel coverage was 93.9±5.4%. All boundaries of the right and left putamen voxels for the 2 sessions encompassed the desired region. The mean putaminal concentrations of metabolites that met our criteria for reliable quantification (CRLB<20%) are summarised in Table 2. Metabolite concentrations in the control group were not significantly different between the right and left putamen. We therefore, considered the averaged concentrations from both sides in further statistical analysis. At baseline, major metabolites (tNAA, tCr, tCho and the pool of the Glu and Gln (Glx)) concentrations in the putamen contralateral to the more affected hemibody of PD patients tended to be much lower than that of controls. However, data were not significantly different (Table 2; tNAA: 8.4±0.3 mM vs. 9.0±0.2 mM, ns, z = -1.46, p = 0.145; tCho: 2.2±0.1 mM vs. 2.4±0.04 mM, ns, z = -1.25, p = 0.212; tCr: 8.6±0.3 mM vs. 9.2±0.2 mM, ns, z = -1.39, p = 0.163; Glx: 14.7±1.1 mM vs. 16.4±0.2 mM, ns, z = -1.22, p = 0.2). Then, they have been normalized to the control levels during the subsequent follow-up visit. Interestingly, at baseline, PD patients had significantly higher Glu and Gln levels in the putamen ipsilateral to the more affected hemibody than contralateral to it (Fig. 3; Glu: 12.2±0.6 mM vs. 10.4±0.6 mM, p<0.05, z = 2.38, p = 0.017; Gln: 6.0±0.4 mM vs. 4.8±0.4 mM, p<0.05, z = 2.55, p = 0.011). This asymmetry disappeared at Visit 2 (Glu: 12.3±0.3 mM vs. 10.9±0.6 mM, ns, z = 0.41, p = 0.684; Gln: 6.2±0.3 mM vs. 5.6±0.4 mM, ns, z = 0.60, p = 0.546). Only the Gln concentration in the ipsilateral putamen was significantly higher in PD patients than in controls at both visits (Visit 1: 6.0±0.4 mM vs. 5.2±0.2 mM, p<0.05, z = 1.98, p = 0.048 and Visit 2: 6.2±0.3 mM vs. 5.2±0.2 mM, p<0.05, z = 2.02, p = 0.044). The pool of the two metabolites (Glx) assessed in PD patients was also significantly higher in the putamen ipsilateral to the more affected hemibody than contralateral to it (Glx: 17.9±0.8 mM

vs. 14.7±1.1 mM, $p<0.05$, $z = 2.52$, $p = 0.012$). This asymmetry persisted at the second visit (Glx: 18.3±0.6 mM vs. 16.1±0.9 mM, $p<0.01$, $z = 3.17$, $p = 0.002$).

There were no significant correlations between the metabolite concentrations and either the UPDRS scores (part III), Hoehn & Yahr stages or the Schwab & England scores.

DISCUSSION

In this longitudinal study, we used ^{1}H MRS at 3 T to investigate concentrations of metabolites *in vivo* in the putamen of both hemispheres of patients at early symptomatic stages of PD and the evolution of these neurochemical profiles. Looking at differences according to the side of motor manifestation predominance, it was interesting to notice that the major metabolites (tNAA, tCho, tCr and Glx) concentrations in the contralateral putamen of PD patients at baseline visit tended to be much lower than that of control subjects. Values had been normalized to the control levels during the subsequent follow-up visit. This observation, in particular, the reduction of tNAA and tCr in contralateral putamen of PD patients and their recovery after antiparkinsonian therapy were consistent with our previous report [14]. The lack of significance could be explained by the fact that the evaluations are carried out at different stages of the disease course.

To our knowledge, only one study presenting ^{1}H MRS results in absolute concentrations of metabolites reports elevated pontine and putaminal GABA levels in mild-moderate PD [21]. These high GABA levels could reflect a hyperactivity of striatal GABAergic neurons in response to nigrostriatal denervation, consistent with immunochemical and electrophysiological data obtained in 6-OHDA-lesioned rats [22]. Unlike these studies, we found no change in GABA concentration in the putamen of *de novo* PD patients. Although methodological issues (disease stage, target brain region/side, magnetic field strength, and low brain GABA concentration) could account for such discrepancy, one possible explanation is a less striatal dopamine denervation in *de novo* patients, below a threshold for triggering changes in GABA levels.

Pooling Glu and/or Gln concentrations measured in contralateral and ipsilateral putamen, our results are consistent with previous studies that report no difference in striatal Glu and Gln levels between

patients and controls [14,21,23]. However, the present study provides new insights in the putaminal glutamatergic metabolism dysfunction in PD according to the predominance of motor signs. PD motor symptoms have an asymmetrical presentation at onset in most patients, as also observed here, and although spreading to both sides as the disease evolves, symptom asymmetry usually persists at later stages [24]. This clinical lateralization has been related to an asymmetry of the damage to the nigrostriatal dopamine system [25]. By considering the two sides separately, our work demonstrates an asymmetry in the changes of Glu and Gln in the putamen. Surprisingly, levels of these metabolites were elevated in the side ipsilateral to the major clinical signs, presumed to be the less affected striatal side, versus the contralateral side, and for Gln, versus controls. This is not what was expected from data obtained in animal models with unilateral massive dopaminergic loss. Many *in viv*o MRS and *ex -vivo* studies in these models demonstrated elevated striatal concentrations of Glu and Gln, consistent with morphofunctional evidences for increased glutamate transmission and compensatory mechanisms to prevent excitotoxicity [4,7,26], but this hyper-glutamatergy is usually described in the striatum with extensive dopaminergic denervation. Our present data seem robust, because these high levels were observed at both visits, but they are still not fully explained. First, we can't totally exclude the fact that the number of PD patients at baseline and visit 2 was different (17 vs. 14) could induce a bias. The use of random-effects models for statistical analysis can however limit it. Then, previous studies in unilateral 6-OHDA lesioned rat models of PD reported bilateral microstructural and metabolic alterations in the striatum, suggesting interhemispheric adaptive mechanisms including bilateral changes in striatal monoamine levels and turnover [27]. Crabbe et al [28] showed time-constant and levodopa treatment independent higher Gln concentration in the contralateral putamen of 6-OHDA rats and no change in the striatum of the side of the 6-OHDA injection. There is therefore a lack of direct correlation between the side of dopaminergic neurons lesion and the level of glutamatergic metabolites. This might be due, at least in part, to the interhemispheric projections from the substantia nigra pars compacta to the striatum [29]. In our study, the absence of modification on the more affected side could be linked to

compensatory mechanisms and adaptability. Classic compensatory mechanisms have been attributed to changes in the nigro-striatal system, such as increased neuronal activity in the substantia nigra pars compacta and enhanced dopamine synthesis and release in the striatum. As discussed by Blesa et al. in their review in 2017 [30], our results and hypothesis could argue in favour of adaptive circuit changes within the basal ganglia and their connections. The contralateral less affected hemisphere may also play a compensatory role for dopaminergic depletion of the more affected hemisphere in PD.

Another explanation would involve glutamatergic projections to the striatum. Besides the corticostriatal input, the striatum also receives heavy glutamatergic projections from the centre median-parafascicular (CM/Pf) complex of the thalamus. Post-mortem studies have shown that 30-40% of the CM/Pf neurons are lost in PD, suggesting that this degeneration might be a primary phenomenon [31]. Because MRS assesses intracellular and synaptic Glu, the loss of thalamic glutamatergic inputs to the striatum may outweigh reactive changes in corticostriatal transmission at early stages especially in the more severely affected side. There is also evidence that Glu and GABA might be co-transmitters of the nigrostriatal system, making further complexifying the interpretation of changes in these transmission systems under progressive asymmetrical degeneration of this pathway. The striatum also receives sparse glutamatergic projections from the subthalamic nucleus [32], whose reactivity in early PD stages remains to be investigated. Furthermore, little is known about the reactivity of the contralateral corticostriatal projections, which though sparse compared with the prevalent ipsilateral component, might play a role in the cascade of changes elicited by the degenerative process. Finally, our results support the Foffani et Obeso's theory [33]. They propose that corticostriatal activity may represent a critical somatotopic ''stressor'' for nigrostriatal terminals, ultimately driving retrograde nigrostriatal degeneration and leading to focal motor onset and progression of PD. This glutamatergic hyperactivity could come before dopaminergic degeneration and therefore it would be visible on the side least affected in the early stages.

Previously, we demonstrated that levodopa administration in PD patients restored tNAA and tCr levels close to control values [14]. Furthermore, in PD animal models, we showed that glutamate and glutamine levels were normalised after acute levodopa administration [8]. Here, the establishment of an antiparkinsonian treatment did not modify the metabolite concentrations versus those measured in patients at baseline without treatment, further supporting the view that non-dopaminergic mechanisms might contribute to the changes in Glu metabolism in patients at early PD stage. However, we cannot exclude the hypothesis that dopaminergic treatment normalized some altered metabolite levels associated with the disease's progression. Only the MRS acquisitions in OFF treatment situation during session 2 would have made it possible to conclude. Furthermore, only three patients received levodopa and the other 11 patients had dopaminergic agonists alone. This point can also explain the lack of change in Glu and Gln levels.

No significant correlations between putaminal MRS findings and clinical motor scores were found, in line with major previous studies [12,23]. The lack of correlation between Glx levels and clinical scores may also be due to the similarity of the clinical stage of our patients and its modest evolution between the two visits. In future investigations, it would also be useful to have larger groups of patients in a wider range of disease stages.

CONCLUSION

By differentiating the ipsilateral and contralateral putamen relative to the predominance of motor damage, the present study demonstrates an elevation of Gln, Glu levels in the putamen ipsilateral to the more affected hemibody in *de novo* PD patients, suggesting the occurrence of interhemispheric adaptive changes in glutamate metabolism. Like other ^{1}H MRS studies in humans, we do not find, at the level of the striatum the more depleted in dopamine, the metabolic changes well established in animal models of PD. These findings could challenge the models of basal ganglia dysfunction in the PD state based on data obtained in animal models that mimic dopamine loss but do not reproduce the progressive character of the degeneration and the multiplicity of cell types affected in

the central and peripheral nervous system [34]. They could point to the involvement of adaptive circuit changes within the basal ganglia and related structures limiting glutamatergic hyperactivity in early symptomatic PD stages.

AUTHOR CONTRIBUTIONS

Conceived and designed the experiments: CC FD. Performed the experiments: CC AC CT BD AM FD ST. Analysed the data: FB CC BP. Wrote the paper: CC FD FB ST.

Acknowledgements: This work was supported by grants from the University Hospital of Clermont-Ferrand. We thank Dr Lydia Kerkerian-Le Goff for her help and advice in writing the manuscript.

REFERENCES

[1] J. Jancovik, Parkinson's disease: clinical features and diagnosis. J Neurol Neurosurg Psychiatry 79 (2008) 368-376, https://doi.org/10.1136/jnnp.2007.131045.

[2] R.M. Villalba, A. Mathai, Y. Smith, Morphological changes of glutamatergic synapses in animal models of Parkinson's disease. Front Neuroanat 9 (2015) 117, https://doi.org/10.3389/fnana.2015.00117.

[3] P. Anglade, A. Mouatt-Prigent, Y. Agid, et al., Synaptic plasticity in the caudate nucleus of patients with Parkinson's disease. Neurodegeneration 5 (1996) 121-8, https://doi.org/ 10.1006/neur.1996.0018.

[4] R.M. Villalba, Y. Smith, Neuroglial Plasticity at Striatal Glutamatergic Synapses in Parkinson's Disease. Frontiers in Systems Neuroscience 5 (2011) 68, https://doi.org/10.3389/fnsys.2011.00068.

[5] B. Picconi, A. Pisani, I. Barone, P. Bonsi, D. Centonze, G. Bernardi G, et al., Pathological Synaptic Plasticity in the Striatum: Implications for Parkinson's Disease. NeuroToxicology 26 (2005) 779–783, https://doi.org/10.1016/j.neuro.2005.02.002.

[6] V. Paille, B. Picconi, V. Bagetta, V. Ghiglieri, C. Sgobio, M. Di Filippo, et al., Distinct Levels of Dopamine Denervation Differentially Alter Striatal Synaptic Plasticity and NMDA Receptor Subunit Composition. J. Neurosci. (2010) 30 14182-14193, https://doi.org/10.1523/JNEUROSCI.2149-10.2010.

[7] C.K. Meshul, J.P. Cogen, H.W. Cheng, C. Moore, L. Krentz, T.H. McNeill, Alterations in Rat Striatal Glutamate Synapses Following a Lesion of the Cortico- And/or Nigrostriatal Pathway. Experimental Neurology (2000) 165 191–206, https://doi.org/10.1006/exnr.2000.7467.

[8] C. Chassain, G. Bielicki, C. Keller, J.P. Renou, F. Durif, Metabolic changes detected in vivo by ^{1}H MRS in the MPTP-intoxicated mouse. NMR Biomed. 23 (2010) 547-53, https://doi.org/10.1002/nbm.1504.

[9] C. Melon, C. Chassain, G. Bielicki, J.P. Renou, L. Kerkerian-Le Goff, P. Salin, et al., Progressive brain metabolic changes under deep brain stimulation of subthalamic nucleus in parkinsonian rats. J Neurochem 132 (2015) 703-12, https://doi.org/10.1111/jnc.13015.

[10] C. Chassain, C. Melon, P. Salin, F. Vitale, S. Couraud, F. Durif et al., Metabolic, synaptic and behavioral impact of 5-week chronic deep brain stimulation in hemiparkinsonian rats. J Neurochem (2016) 136 1004-16, https://doi.org/10.1111/jnc.13438.

[11] C. Lucetti, P. Del Dotto, G. Gambaccini, S. Bernardini, M.C. Bianchi, M. Tosetti, et al., Proton magnetic resonance spectroscopy (1H-MRS) of motor cortex and basal ganglia in de

novo Parkinson's disease patients. Neurol Sci (2001) 22 69-70, https://doi.org/10.1007/s100720170051.

[12] R. Camicioli, J.R. Korzan, S.L. Foster, N.J. Fisher, D.J. Emery, A.C. Bastos, et al., Posterior cingulate metabolic changes occur in Parkinson's disease patients without dementia. Neurosci Lett (2004) 354 177– 180, https://doi.org/10.1016/j.neulet.2003.09.076.

[13] K. Nie, Y. Zhang, B. Huang, L. Wang, J. Zhao, Z. Huang et al., Marked N-acetylaspartate and choline metabolite changes in Parkinson's disease patients with mild cognitive impairment. Parkinsonism Relat Disord (2013)19 329–334, https://doi.org/10.1016/j.parkreldis.2012.11.012.

[14] L. Mazuel, C. Chassain, B. Jean, B. Pereira, A. Cladière, C. Speziale et al., Proton MR Spectroscopy for Diagnosis and Evaluation of Treatment Efficacy in Parkinson Disease. Radiology (2016) 278, 505-13, https://doi.org/10.1148/radiol.2015142764

[15]. K. Abe, H. Terakawa, M. Takanashi M, Y. Watanabe, H. Tanaka, N. Fujita, et al., Proton magnetic resonance spectroscopy of patients with parkinsonism. Brain Research Bulletin (2000) 52 589–595, https://doi.org/10.1016/s0361-9230(00)00321-x.

[16] B. Toczylowska, E. Zieminska, M. Michałowska, M. Chalimoniuk, U. Fiszer, Changes in the metabolic profiles of the serum and putamen in Parkinson's disease patients – In vitro and in vivo NMR spectroscopy studies. Brain Research (2000) 1748 147118, https://doi.org/10.1016/j.brainres.2020.147118.

[17] A. Hughes, S.E. Daniel, L. Kilford, A.J. Lees, Accuracy of clinical diagnosis of idiopathic Parkinson's disease. A clinico-pathological study of 100 cases. J Neurol Neurosurg Psychiatry (1992) 55, 181–184, https://doi.org/10.1136/jnnp.55.3.181.

[18] C.L. Tomlinson, R. Stowe, S. Patel, C. Rick, R. Gray, C.E. Clarke, Systematic review of levodopa dose equivalency reporting in Parkinson's disease. Movement Disord (2010) 25 2649 2653, https://doi.org/10.1002/mds.23429.

[19] M. Wilson, O. Andronesi, P.B. Barker, R. Bartha, A. Bizzi, P.J., K.M. Brindle, et al., Methodological consensus on clinical proton MRS of the brain: Review and recommendations. Magn Reson Med (2019) 82 527-550, https://doi.org/10.1002/mrm.27742.

[20] S.W. Provencher, Estimation of metabolite concentrations from localized in vivo proton NMR spectra. Magn Reson Med (1993) 30 672–679, https://doi.org/10.1002/mrm.1910300604.

[21] U.E. Emir, P.J. Tuite, G. Öz, Elevated pontine and putamenal GABA levels in mild-moderate Parkinson disease detected by 7 Tesla proton MRS. PloSONE (2012) 7 1–7, https://doi.org/10.1371/journal.pone.0030918.

[22] A.R. Carta, S. Fenu, P. Pala, E. Tronci, M. Morelli, Selective modifications in GAD67 mRNA levels in striatonigral and striatopallidal pathways correlate to dopamine agonist priming in 6-

hydroxydopamine-lesioned rats. Eur J Neurosci (2003) 18 2563–2572, https://doi.org/10.1046/j.1460-9568.2003.02983.x.

[23] N. Weiduschat, X. Mao, M.F. Beal, M.J. Nirenberg, D.C. Shungu, C. Henchcliffe, Usefulness of proton and phosphorus MR spectroscopic imaging for early diagnosis of Parkinson's disease. J Neuroimaging 25 (2013) 105–110, https://doi.org/10.1111/jon.12074.

[24] M.J. Barrett, S.A. Wylie, M.B. Harrison, G.F. Wooten GF, Handedness and motor symptom asymmetry in Parkinson's disease. J Neurol Neurosurg Psychiatry 82 (2011) 1122-1124, https://doi.org/10.1136/jnnp.2010.209783.

[25] W.S, .Huang, S.Z. Lin, J.C. Lin, S.P. Wey, G. Ting, R.S. Liu, Evaluation of early-stage Parkinson's disease with 99mTc-TRODAT-1 imaging. J Nucl Med (2001) 42 1303-1308,

[26] P.G. Coune, M. Craveiro, M.N. Gaugler, V. Mlynárik, B.L. Schneider, P. Aebischer, et al., An in vivo ultrahigh field 14.1 T (1) H-MRS study on 6-OHDA and alpha-synuclein-based rat models of Parkinson's disease: GABA as an early disease. NMR Biomed 26 (2013) 43–50. https://doi.org/10.1002/nbm.2817.

[27] M. Pierucci, V. Di Matteo, A. Benigno, G. Crescimanno, E. Esposito, G. Di Giovanni, The unilateral nigral lesion induces dramatic bilateral modification on rat brain monoamine neurochemistry. Ann NY Acad Sci (2009) 1155, 316e323, https://doi.org/10.1111/j.1749-6632.2008.03679.x

[28] M. Crabbé, A. Van der Perren, A. Weerasekera, U. Himmelreich, V. Baekelandt, K. Van Laere, C. Casteels, Altered mGluR5 binding potential and glutamine concentration in the 6-OHDA rat model of acute Parkinson's disease and levodopa-induced dyskinesia. Neurobiology of Aging (2018) 61 82e92, https://doi.org/10.1016/j.neurobiolaging.2017.09.006.

[29] S. Morgan, J.P. Huston, The interhemispheric projection from the substantia nigra to the caudate-putamen as depicted by the anterograde transport of [3H] leucine. Behav. Brain Res (1990) 38 155e162. https://doi.org/10.1016/0166-4328(90)90013-5.

[30] R. Blesa, I. Trigo-Damas, M. Dileone, N. Lopez-Gonzalez del Rey, L.F. Hernandez, J.A. Obeso, Compensatory mechanisms in Pa.rkinson's disease: Circuits adaptations and role in disease modification. Experimental Neurology (2017) 298 148-161, https://doi.org/10.1016/j.expneurol.2017.09.006.

[31] J.M. Henderson, K. Carpenter, H. Cartwright, G.M. Halliday, Degeneration of the centré median-parafascicular complex in Parkinson's disease. Ann Neurol (2000) 47 345-52.

[32] A. Emmi, A. Antonini, V. Macchi, A. Porzionato, R. De Caro, Anatomy and Connectivity of the Subthalamic Nucleus in Humans and Non-human Primates. Front Neuroanat (2020) 14 13, https://doi.org/10.3389/fnana.2020.00013.

[33] G. Foffani, J.A. Obeso, A Cortical Pathogenic Theory of Parkinson's Disease. Neuron (2018) 99 1116-1128, https://doi.org/10.1016/j.neuron.2018.07.028.

[34] J.A. Obeso, J.L. Lanciego, Past, present, and future of the pathophysiological model of the Basal Ganglia. Front Neuroanat (2011) 5 39, https://doi.org/10.3389/fnana.2011.00039.

FIGURE LEGENDS

Fig. 1. T1 weighted images of a de novo PD patient with the volume of interest ($10 \times 30 \times 15 mm^3$) in the right putamen (top) and in the left putamen (bottom) for localised ^{1}H-MRS

A-P: anterio-posterior; R-L: right-left; D-V: dorsal-ventral.

Fig. 2. Representative ^{1}H-MR spectrum acquired with the PRESS sequence at 3T (TE/TR = 29 ms/1500 ms, 512 averages)

The corresponding LCModel spectral fit, fit residual, some individual metabolite, macromolecules, and baseline fits are presented. Metabolite fits are assigned as follows: total N-acetyl-aspartate (tNAA = sum of NAA and NAAG), total creatine (tCr = sum of Cr and PCr), total choline (tCho = sum of GPC and PCh), glutamate (Glu), glutamine (Gln), gamma-aminobutyric acid (GABA), inositol (Ins) and taurine + glucose (Tau).

Fig. 3. Scatter plot of glutamine (Gln), glutamate (Glu), and glutamate + glutamine (Glx) concentrations measured on ^{1}H spectra in the putamen ipsi- and contralateral to the more affected hemibody of PD patients and right, left and mean concentrations for controls

Black and grey circles are concentrations for 17 PD patients at Visit 1 and 14 PD patients at Visit 2. Concentrations are measured in the putamen ipsilateral (black) and contralateral (grey) to the major clinical parkinsonian signs. For control group, as the data are not significantly different between left and right putamen, the values obtained for each side are averaged. Total blue markers stand for 17 controls. Bars are the means. Metabolite are assigned as follows: glutamate (Glu), glutamine (Gln), glutamate + glutamine (Glx).

*$p < 0.05$, **$p < 0.01$ vs. contralateral putamen and # $p < 0.05$ vs. control.

Table 1. Demographics and clinical characteristics of the subjects

Abbreviations: Sex: F =female, M =male; PD: Parkinson's disease; UPDRS: unified Parkinson's disease rating scale; UPDRS-III: scores on the unified Parkinson's disease rating scale motor evaluation.

Values are means ± SEM. Comparison of Control and PD subjects' ages was performed using Student's t-test. Comparisons of clinical data (i.e. between visit 1 and visit 2 for PD) were performed using paired Student's t-test. Significant ($p < 0.05$) were assigned as ###$p < 0.001$ for UPDRS-III sub-score on side of PD onset *vs.* the other side.

Table 2. Absolute concentrations of metabolites (mean ± SEM in mmol.L-1) for the different groups

Metabolites concentrations in the control group were not significantly different between the right and the left putamen, then data are the mean from both sides. In PD patients at the first visit, Glu and Gln concentrations were significantly higher in the putamen ipsilateral to the more affected hemibody than in that contralateral to it. This was the case only for the pool Glu+Gln in the second visit. There was no difference between groups when concentrations represented the average on the two sides. On the other hand, the Gln levels measured in the putamen ipsilateral to the more affected hemibody were significantly higher in Parkinson patients during their two visits compared with the controls.

* represent results of the random-effect model used to compare absolute concentrations of metabolites between healthy subjects and PD patients and to take account matching (pair as random-effect): *$p < 0.05$ ipsilateral vs. contralateral.

‡ represent results of the random-effect model used to compare absolute concentrations of metabolites between visit 1 and visit 2 for PD patients and to take account between and within patient variability and between and within side effect (patient and side as random-effects): ‡ $p < 0.05$ control group (mean values) vs. PD patients ipsilateral Visit 1 and Visit 2.

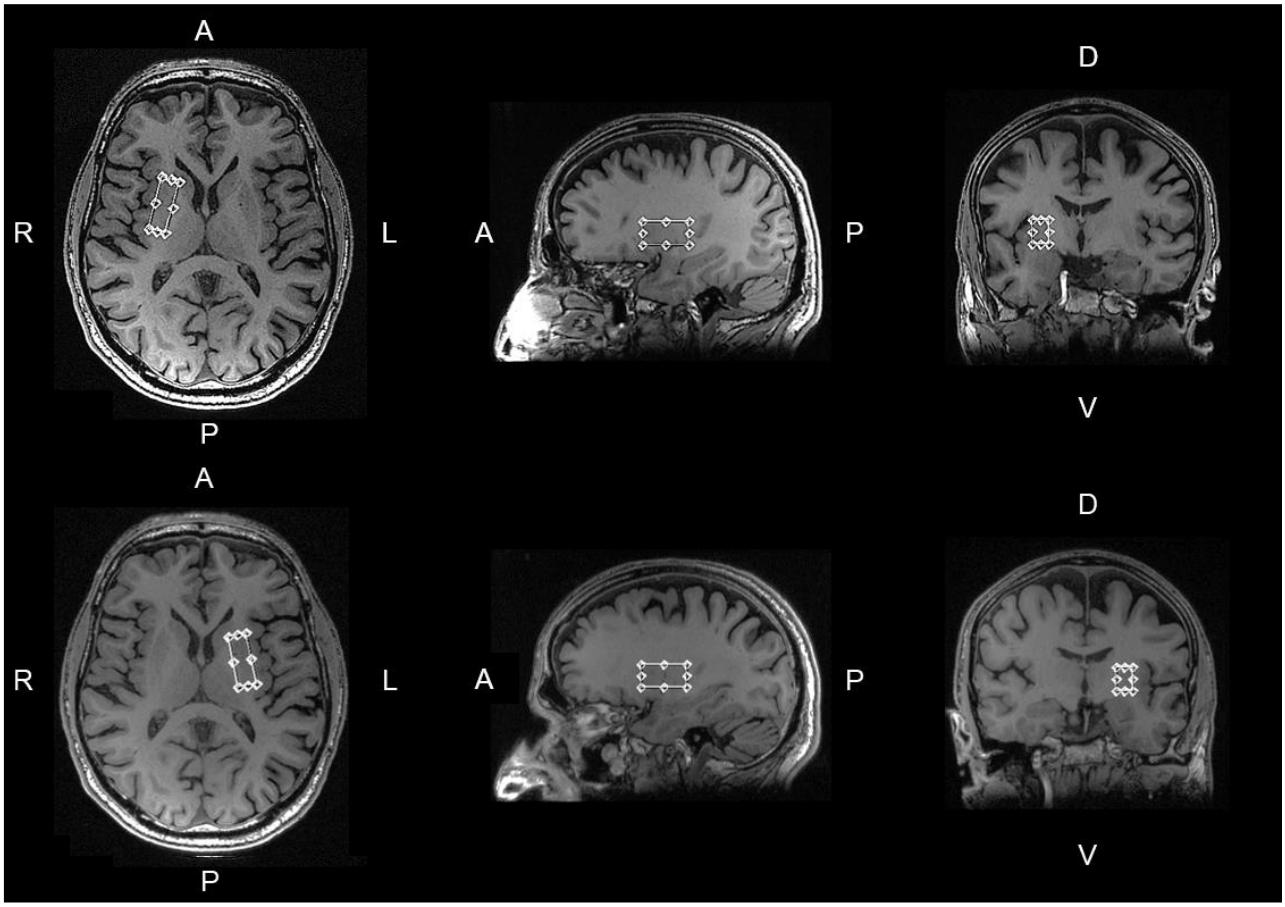

Fig. 1. T1 weighted images of a de novo PD patient with the volume of interest (10 × 30 × 15mm^3) in the right putamen (top) and in the left putamen (bottom) for localised ^{1}H-MRS

A-P: anterior-posterior; R-L: right-left; D-V: dorsal-ventral.

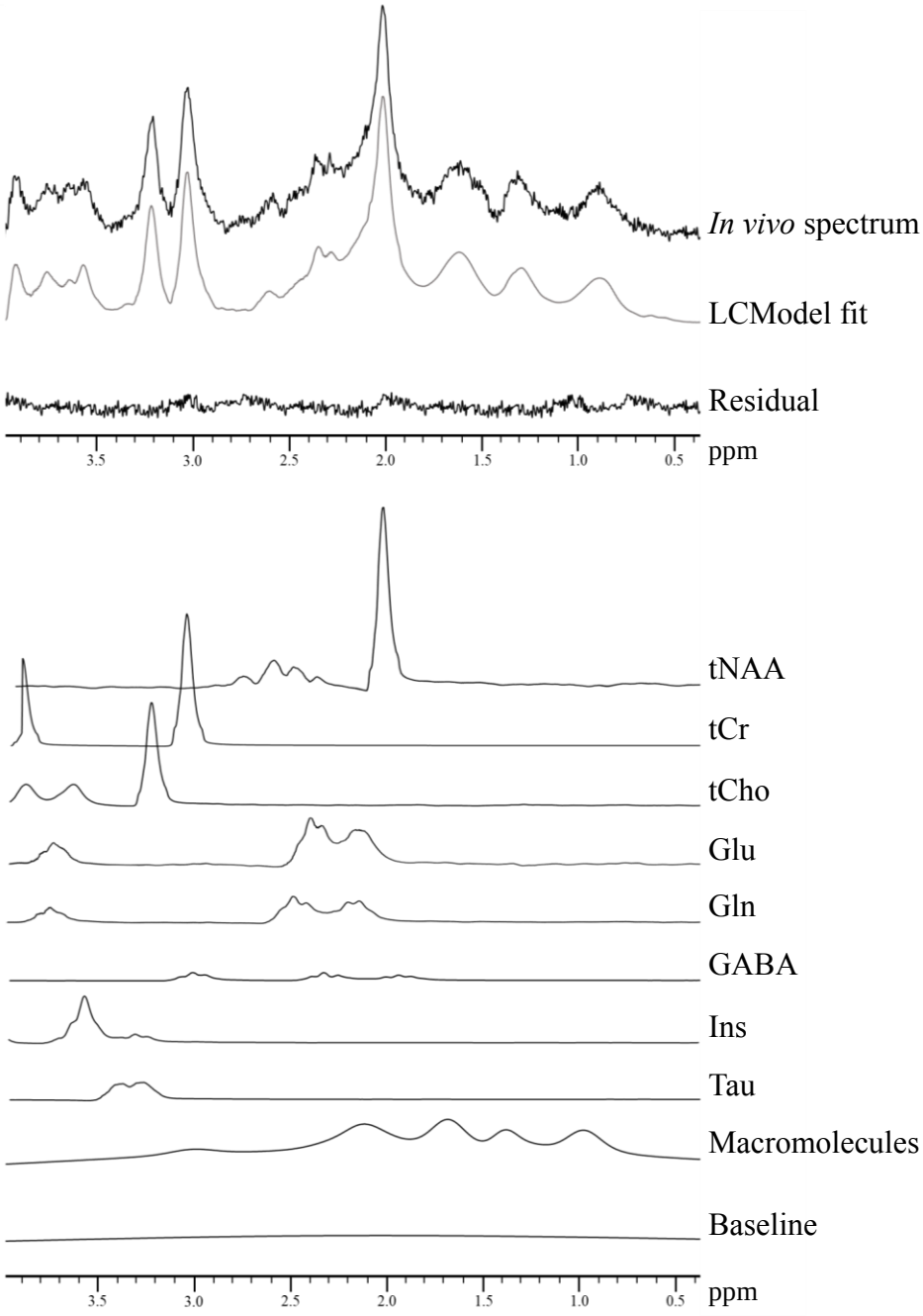

Fig. 2. Representative ^{1}H-MR spectrum acquired with the PRESS sequence at 3T (TE/TR = 29 ms/1500 ms, 512 averages)
The corresponding LCModel spectral fit, fit residual, macromolecules, baseline and individual metabolite fits are presented. Metabolite fits are assigned as follows: total N-acetyl-aspartate (tNAA), total creatine (tCr), total choline (tCho), glutamate (Glu), glutamine (Gln), gamma-aminobutyric acid (GABA), inositol (Ins) and taurine + glucose (Tau).

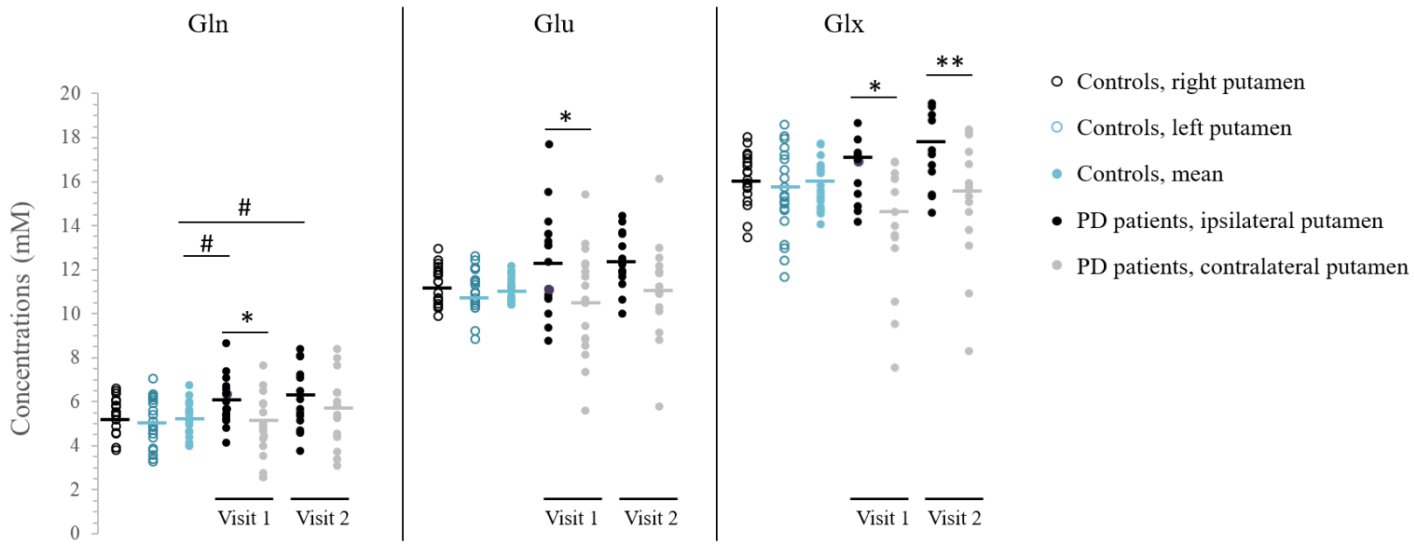

Fig. 3. Scatter plot of glutamine (Gln), glutamate (Glu), and glutamate + glutamine (Glx) concentrations measured on 1H spectra in the putamen ipsi- and contralateral to the more affected hemibody of PD patients and right, left and mean concentrations for controls

Black and grey circles are concentrations for 17 PD patients at Visit 1 and 14 PD patients at Visit 2. Concentrations are measured in the putamen ipsilateral (black) and contralateral (grey) to the major clinical parkinsonian signs. For control group, as the data are not significantly different between left and right putamen, the values obtained for each side are averaged. Total blue markers stand for 17 controls. Bars are the means. Metabolite are assigned as follows: glutamate (Glu), glutamine (Gln), glutamate + glutamine (Glx).

*$p < 0.05$, **$p < 0.01$ vs. contralateral putamen and # $p < 0.05$ vs. control.

TABLE 1. Demographics

	Control (n=17)	**PD (visit 1) (n=17)**	**PD (visit 2) (n=14)**	
	Mean ± SEM	Mean ± SEM	Mean ± SEM	
Age, years	62.7 ± 2.5	64.3 ± 2.4	68.0 ± 2.3	t(16) = 1.24; p = 0.12
Gender (F/M)	5/12	5/12	2/12	—
Duration of PD, months	—	16.5 ± 3.5	53.4 ± 2.0	—
Age at PD onset, years	—	62.8 ± 2.5	64.9 ± 2.4	—
Delay between visit 1 and visit 2, months	—	—	36.9 ± 2.1	—
L-Dopa equivalent daily dose (LEDD) (mg)	—	—	444 ± 13.9	—
UPDRS total score	—	19 ± 2.4	21.1 ± 2.6	t(26) = 0.57; p = 0.29
UPDRS-III motor score	—	14.8 ± 2.1	19.5 ± 1.3	t(26) = 0.68; p = 0.25
Side of PD onset	—	14 right / 3 left		
UPDRS-III motor sub-score on the predominant side of PD onset vs the other side	—	predominant signs: 10.1 ± 1.4 vs. 2.4 ± 0.6$^{###}$; t(16) = 5.47; p=0.00003	predominant signs: 12.6 ± 2.1 vs. 4.2 ± 0.9$^{###}$; t(16) = 5.09; p=0.0001	
Hoehn & Yahr stage	—	1.5 ± 0.1	1.6 ± 0.1	t(26) = 0.48; p = 0.32
Schwab & England score, %	—	89 ± 1.5	92.5 ± 1.3	t(26) = 0.99; p = 0.16

Table 1. Demographics and clinical characteristics of the subjects
Abbreviations: Sex: F female, M male; PD: Parkinson's disease; UPDRS: unified Parkinson's disease rating scale; UPDRS-III: scores on the unified Parkinson's disease rating scale motor evaluation.
Values are means ± SEM. Comparison of Control and PD subjects' ages was performed using Student's t-test. Comparisons of clinical data (i.e. between visit 1 and visit 2 for PD) were performed using paired Student's t-test. Significant ($p < 0.05$), were assigned as ###$p < 0.001$ for UPDRS-III sub-score on side of PD onset *vs.* the other side.

Metabolites	Control (n=17)			PD patients visit 1 (n=17)			PD patients visit 2 (n=14)		
	Right	Left	Mean	Ipsilateral	Contralateral	Mean	Ipsilateral	Contralateral	Mean
GABA	1.05 ± 0.09	1.10 ± 0.15	1.07 ± 0.03	1.08 ± 0.09	1.03 ± 0.05	1.06 ± 0.02	0.99 ± 0.04	0.96 ± 0.03	0.98 ± 0.02
Gln	5.17 ± 0.73	5.44 ± 0.61	5.31 ± 0.16 ‡	5.99 ± 0.41 *	4.79 ± 0.35	5.39 ± 0.42	6.15 ± 0.31	5.60 ± 0.43	5.88 ± 0.33
Glu	11.26 ± 0.63	10.90 ± 0.66	11.08 ± 0.14	12.16 ± 0.57 *	10.38 ± 0.58	11.27 ± 0.63	12.26 ± 0.28	10.92 ± 0.61	11.59 ± 0.60
Ins	6.56 ± 0.52	6.27 ± 0.69	6.41 ± 0.14	6.17 ± 0.50	6.05 ± 0.32	6.11 ± 0.05	6.81 ± 0.22	6.48 ± 0.39	6.64 ± 0.12
Tau	2.54 ± 0.67	214 ± 1.33	2.34 ± 0.38	2.37 ± 0.54	2.48 ± 0.39	2.43 ± 0.04	2.57 ± 0.47	3.19 ± 0.76	2.88 ± 0.22
tNAA	9.64 ± 0.89	8.403 ± 0.97	9.04 ± 0.24	8.91 ± 0.43	8.40 ± 0.27	8.66 ± 0.18	9.47 ± 0.47	9.40 ± 0.37	9.44 ± 0.08
tCho	2.40 ± 0.18	2.31 ± 0.19	2.35 ± 0.04	2.32 ± 0.09	2.20 ± 0.07	2.26 ± 0.04	2.58 ± 0.12	2.34 ± 0.18	2.45 ± 0.08
tCr	9.39 ± 0.73	9.01 ± 0.89	9.20 ± 0.17	9.06 ± 0.31	8.63 ± 0.26	8.84 ± 0.15	9.29 ± 0.27	9.23 ± 0.38	9.25 ± 0.02
Glx	16.38 ±1.03	16.34 ±1.25	16.36 ± 0.24	17.90 ± 0.77 *	14.70 ± 1.06	16.30 ± 1.31	18.27 ± 0.56 *	16.06 ± 0.87	17.16 ± 0.78

Table 2. Absolute concentrations of metabolites (mean ± SEM in $mmol.L^{-1}$) for the different groups

Metabolites concentrations in the control group were not significantly different between the right and the left putamen, then data are the mean from both sides. In PD patients at the first visit, Glu and Gln concentrations were significantly higher in the putamen ipsilateral to the more affected hemibody than in that contralateral to it. This was the case only for the pool Glu+Gln in the second visit. There was no difference between groups when concentrations represented the average on the two sides. On the other hand, the Gln levels measured in the putamen ipsilateral to the more affected hemibody were significantly higher in Parkinson patients during their two visits compared with the controls.

* represent results of the random-effect model used to compare absolute concentrations of metabolites between healthy subjects and PD patients and to take account matching (pair as random-effect): *$p < 0.05$ ipsilateral *vs.* contralateral.

‡ represent results of the random-effect model used to compare absolute concentrations of metabolites between visit 1 and visit 2 for PD patients and to take account between and within patient variability and between and within side effect (patient and side as random-effects: ‡ $p < 0.05$ control group (mean values) *vs*. PD patients ipsilateral Visit 1 and Visit 2.